AD-A111 274 SAN DIEGO STATE UNIV CA DEPT OF AEROSPACE ENGINEERIN--ETC F/G 11/3
COMPLIANT-COATING-FLUID INTERACTION: COATING LONGITUDINAL WAVES--ETC(U)
FEB 82 M PIERUCCI, P A BAXLEY N00014-81-K-0424
UNCLASSIFIED AE/EM-TR-82-04 NL

1 OF 1
AD A
111 274

END
DATE
FILMED
03-82
DTIC

(12)

AE&EM TR-82-04

AD A111274

COMPLIANT-COATING-FLUID INTERACTION: COATING LONGITUDINAL WAVES IN STATIONARY FLUID

Mauro Pierucci
Paul A. Baxley

FEB 2 5 1982

E

February 1982

Research Sponsored by Office of Naval Research under Contract N00014-81-K-0424

Approved for Public Release – Distribution Unlimited

SAN DIEGO STATE UNIVERSITY
College of Engineering
Department of Aerospace Engineering
and Engineering Mechanics
San Diego, CA 92182-0183
(714) 265-6074

82 02 23 037

ABSTRACT

The presence of a thin non-homogeneous layer at the interface of an elastic and a fluid medium can alter the energy exchange between the two media. In this report the effect of the transition layer upon the propagation of one-dimensional longitudinal waves is analyzed. The motion of the lower boundary of the elastic layer is assumed known and the energy radiation into the fluid is obtained.

TABLE OF CONTENTS

1 - INTRODUCTION

In a previous report[1] it has been shown that under certain sets of conditions, a thin non-homogeneous viscoelastic layer interposed between an elastic solid and a viscous fluid can change the resonance characteristics of the elastic layer. The interest of this report is to analyze the same system studied in reference 1 acting under the influence of a longitudinal one-dimensional disturbance (Fig. 1). The longitudinal disturbance is created at the lower boundary of the elastic layer. Coatings and transition layers of interest will have densities close to that of the surrounding fluid (water).

The transition layer can be considered to be either a physical coating interposed between the elastic layer and the fluid or it can be assumed to have an effective thickness with properties related to the mean location of the solid-fluid interface. These properties can be obtained by averaging the location of the interface as a function of both time and space.

II - ANALYSIS

II-1 - Derivation of Governing Equations

The general governing equations for a plane strain motion of a generalized medium are[2]

$$\rho \frac{Dv_1}{Dt} = \frac{\partial \tau_{11}}{\partial x} + \frac{\partial \tau_{12}}{\partial y} \quad , \tag{1}$$

$$\rho \frac{Dv_2}{Dt} = \frac{\partial \tau_{21}}{\partial x} + \frac{\partial \tau_{22}}{\partial y} \quad , \tag{2}$$

$$\frac{D\rho}{Dt} + \rho \left(\frac{\partial v_1}{\partial x} + \frac{\partial v_2}{\partial y}\right) = 0 \quad , \tag{3}$$

where v_1 and v_2 are the velocities in the x and the y direction respectively. The material derivative can be written in terms of v_1 and v_2 :

$$\frac{D}{Dt} = \frac{\partial}{\partial t} + v_1 \frac{\partial}{\partial x} + v_2 \frac{\partial}{\partial y} \quad . \tag{4}$$

The stresses τ_{ij} are related to either the strain or the rate of change of the strain depending upon whether the medium is a solid or a fluid. The general values of the stresses are given by

$$\tau_{11}\Big|_{solid} = \frac{2G}{1-2\nu} \left[(1-\nu) \frac{\partial u_1}{\partial x} + \nu \frac{\partial u_2}{\partial y}\right] \quad , \tag{5}$$

$$\tau_{11}\Big|_{fluid} = -p + \mu\left[\frac{4}{3} \frac{\partial v_1}{\partial x} - \frac{2}{3} \frac{\partial v_2}{\partial y}\right] \quad , \tag{6}$$

$$\tau_{12}\Big|_{solid} = G\left[\frac{\partial u_1}{\partial y} + \frac{\partial u_2}{\partial x}\right] \quad , \tag{7}$$

$$\tau_{12}\Big|_{fluid} = \mu\left[\frac{\partial v_1}{\partial y} + \frac{\partial v_2}{\partial x}\right] \quad , \tag{8}$$

$$\tau_{22}\Big|_{solid} = \frac{\partial G}{1-2\nu}\left[\nu \frac{\partial u_1}{\partial x} + (1-\nu)\frac{\partial u_2}{\partial y}\right] \quad , \tag{9}$$

$$\tau_{22}\Big|_{fluid} = -p + \mu\left[-\frac{2}{3}\frac{\partial v_1}{\partial x} + \frac{4}{3}\frac{\partial v_2}{\partial y}\right] \quad , \tag{10}$$

where u_i are the particle displacements in the i direction. For one-dimensional (i.e. $\frac{\partial}{\partial x} = 0$), longitudinal (i.e. $u_1 = v_1 = 0$), steady-state (i.e. $e^{-i\omega t}$ time dependence) motion with zero mean flow field the governing equations reduce to

$$\rho\left[v_2 \frac{dv_2}{dy} - i\omega v_2\right] = \frac{d}{dy}(\tau_{22}) \quad , \tag{11}$$

$$\frac{d}{dy}(\rho v_2) - i\omega\rho = 0 \quad , \tag{12}$$

with

$$\tau_{22}\Big|_{solid} = \frac{2G(1-\nu)}{1-2\nu}\frac{du_2}{dy} \quad , \tag{13}$$

$$\tau_{22}\Big|_{fluid} = -p - \frac{4}{3} i\mu\omega \frac{du_2}{dy} \quad . \tag{14}$$

For frequencies below ultrasonics, the viscosity term in equation (14) can be neglected. Linearizing equations (11) and (12) will reduce the equations to:

$$\frac{d}{dy}\left(K(y)\frac{du_2}{dy}\right) + \omega^2 u_2 = 0 \quad . \tag{15}$$

K(y) is the generalized stress-strain coefficient and is given by

$$K(y) = \begin{cases} \frac{3(1-\nu)}{(1+\nu)}\frac{k}{\rho} & \text{solid} \\ c_f^2 & \text{fluid} \end{cases} \quad . \tag{16}$$

k is the bulk modulus of the solid. The longitudinal wave speed of the solid c_s is related to the bulk modulus k by

$$c_s^2 = \frac{3k}{\rho} \frac{(1-\nu)}{(1+\nu)} \quad . \tag{17}$$

For a non-homogeneous transition layer with bulk properties varying from that of the solid to that of the fluid, the generalized non-dimensional stress-strain coefficient may be defined by

$$H(y) = K(y)/c_s^2 \quad . \tag{18}$$

Thus

$$H(y) = R + (1-R) \exp[-(y/\ell)^n] \quad , \tag{19}$$

where R is the square of the ratio of the longitudinal velocity of the fluid to that of the elastic solid,

$$R = \left(\frac{c_f}{c_s}\right)^2 \quad . \tag{20}$$

The values of R for different elastic materials immersed in water are shown in Table 1.

Material	R
Steel/Aluminum	0.05
Brass	0.1
Hard Rubber	0.4
ρc Rubber	1.0
Very Soft Rubber	10.0

Table 1 - Values of the square of the ratio of the wave speed in water to that in the solid .

The magnitudes of R of interest are thus seen to vary from 0.05 for very hard material to about 10 for a rubber-like material interlaced with air voids.

The values of n of Eq. (19) are related to the thickness of the transition layer. Small values of n correspond to a thick layer with decreasing thickness as n increases. In the limit as $n \to \infty$ the transition layer disappears and the classic solid-fluid interface is recovered. For $y \ll \ell$ and for any value of n one obtaines the stress-strain coefficient for the elastic solid while for $y \gg \ell$ one recovers the coefficient for the fluid. Fig. 2 shows the effect of different values of n upon the thickness of the transition layer and upon the characteristics of the generalized stress-strain coefficient within the layer.

The differential equation to be solved is

$$\frac{d}{dy}\left(H \frac{du_2}{dy}\right) + \theta_1^2 u_2 = 0 \quad , \tag{21}$$

where θ_1 is the wavenumber in the solid given by

$$\theta_1 = \frac{\omega \ell}{c_s} \quad . \tag{22}$$

The boundary conditions for Eq. (21) are split and are

$$u_2(0) = 1 \quad , \tag{23}$$

$$\lim_{y \to \infty} u_2(y) \longrightarrow \text{outgoing wave} \quad . \tag{24}$$

Note that in the two limits of $y \ll \ell$ and $y \gg \ell$ one obtains

$$u_2'' + \theta_1^2 u_2 = 0 \qquad y \ll \ell \quad , \tag{25}$$

$$u_2'' + \Gamma^2 u_2 = 0 \qquad y \gg \ell \quad , \tag{26}$$

where Γ is the fluid wavenumber and is given by

$$\Gamma = \frac{\omega \ell}{c_f} = \Theta_1/R^{\frac{1}{2}} \quad . \tag{27}$$

For fixed fluid conditions, increasing Γ corresponds to higher frequencies and to thicker solids, while increasing R corresponds to softer solids. Table 2 shows values of Γ for cases of interest.

f \ ℓ	10 cm	1 cm	1 mm
1 Hz	$4\text{x}10^{-4}$	$4\text{x}10^{-5}$	$4\text{x}10^{-6}$
10 Hz	$4\text{x}10^{-3}$	$4\text{x}10^{-4}$	$4\text{x}10^{-5}$
10^2Hz	$4\text{x}10^{-2}$	$4\text{x}10^{-3}$	$4\text{x}10^{-4}$
10^3Hz	0.4	$4\text{x}10^{-2}$	$4\text{x}10^{-3}$
10^4Hz	4	0.4	$4\text{x}10^{-2}$

Table 2 - Values of Γ for different ℓ and frequencies .

As one moves away from the transition layer into the fluid, the validity of Eq. 24 increases. The outer boundary condition is then replaced by a comparison of the numerical solution of Eq. 21 with the outgoing wave solution of Eq. 26;

$$u_2 = Ce^{i\Gamma y} \quad . \tag{28}$$

The numerical integration of Eq. 21 is obtained by a Runge-Kutta procedure. The procedure requires an initial value for $\frac{du_2}{dy}$ at the inner wall; a guess is initially made. The slope at the wall is modified until the numerical solution contains only outgoing waves (i.e. agrees with Eq. 28).

II-2 - Transmission of Longitudinal Waves Through Two Media

In the limit as $n \to \infty$, the transition layer disappears and one obtains the problem of propagation of longitudinal waves from one elastic medium (solid) into another (fluid) (Fig. 3). This limiting solution can be obtained in analytic form and will be used to help understand the numerical results for the transition layer cases.

The propagation of steady-state small vibrations is governed by

$$\rho\omega^2 u_2 + c_s^2 \frac{d^2u_2}{dy^2} = 0 \qquad y<\ell \quad , \tag{29}$$

$$\rho\omega^2 u_2 + c_f^2 \frac{d^2u_2}{dy^2} = 0 \qquad y>\ell \quad . \tag{30}$$

The boundary conditions for these two equations are: (1) unit displacement at lower boundary of solid, (2) equality of displacement at $y=\ell$ (3) equality of stresses at $y=\ell$ and (4) only outgoing waves permitted for $y>\ell$. These four conditions can be expressed by

$$u_2(0) = 1 \quad , \tag{31}$$

$$u_2(\ell)\Big|_{solid} = u_2(\ell)\Big|_{fluid} \quad , \tag{32}$$

$$c_s^2 \frac{du_2(\ell)}{dy}\Bigg|_{solid} = c_f^2 \frac{du_2(\ell)}{dy}\Bigg|_{fluid} \quad , \tag{33}$$

$$u_2(y)\Big|_{fluid} = C\, e^{i\Gamma y} \quad . \tag{34}$$

The solution to Eqs. 29-34 can be shown to be given by

$$u_2(y) = \frac{\cos[\Gamma R^{\frac{1}{2}}(y-\ell)/\ell] - iR^{\frac{1}{2}} \sin[\Gamma R^{\frac{1}{2}}(y-\ell)/\ell]}{\cos(\Gamma R^{\frac{1}{2}}) - iR^{\frac{1}{2}} \sin(\Gamma R^{\frac{1}{2}})} \qquad y<\ell, \tag{35}$$

$$u_2(y) = \frac{\exp[i\Gamma(y-\ell)/\ell]}{\cos(\Gamma R^{\frac{1}{2}}) - i\,R^{\frac{1}{2}}\sin(\Gamma R^{\frac{1}{2}})} \qquad y>\ell\ . \tag{36}$$

The magnitude of the fluid particle displacement u_2 is then given by

$$\left|u_2(y)\right| = [1 + (R-1)\sin^2(\Gamma R^{\frac{1}{2}})]^{-\frac{1}{2}} \quad . \tag{37}$$

For values of R less than unity (i.e. very rigid solids) the particle displacement will be magnified in going from the solid into the fluid. The magnification will be a maximum for

$$\Gamma R^{\frac{1}{2}} = \left(\frac{1+2n}{2}\right)\pi \qquad n = 0,1,2,3,4\ldots\ldots \quad . \tag{38}$$

This condition corresponds to

$$\frac{\ell}{\lambda s} = \frac{1+2n}{4} \qquad n = 0,1,2,3,4\ldots\ldots \quad . \tag{39}$$

Eq. (39) is the condition required for acoustic resonance of a closed-open pipe[3].

For very soft coatings, the value of R will be much greater than unity and the fluid particle displacement will always be less than the wall displacement. The magnitude of the fluid particle displacement will be minimized for

$$\Gamma R^{\frac{1}{2}} = \left(\frac{1+2n}{2}\right)\pi \quad . \tag{38-a}$$

The same condition (Eq. 38) will thus create a fluid particle displacement enhancement and reduction for very rigid and very soft coatings respectively.

Note that for both conditions (very rigid or very soft coatings) for values of

$$\Gamma R^{\frac{1}{2}} = n\pi \qquad n = 0,1,2,3\ldots\ldots \quad , \tag{40}$$

the fluid particle will have exactly the same displacement magnitude as the solid particles; effect of interface is therefore negligible.

In the analysis discussed in this section, for simplicity, it has been assumed that the fluid and the solid densities are equal. Changes in the density ratio will change the quantitative results but will not alter the qualitative aspect discussed above.

III - DISCUSSION OF RESULTS

Figure 4 shows the particle displacement distribution for a particular transition layer thickness (n=8) and for a particular coating material (R=10), as a function of distance from the lower boundary for different Γ's (i.e. different frequencies). As expected, at the lower frequencies the displacement remains unaltered in going from the solid to the fluid (i.e. the longitudinal wave does not see the discontinuity). As the frequency is increased, a more diverse structure in the displacement signature is observed. At a particular frequency, a resonance-type distribution is observed; as frequency is increased further the displacement distribution becomes more uniform again. This type of behavior is very similar to the closed-pipe resonance phenomena discussed previously in the no-transition layer model. Fig. 5 shows the normal stress distribution for the same condition as Fig. 4. The stress distribution as a function of frequency is seen to reflect the resonance phenomena discussed previously.

Figs. 6 and 7 present the particle displacement and the stress distribution at a particular frequency (i.e. Γ=1) for different coatings. The coating material bulk moduli vary from that corresponding to very soft and very rigid rubber. Figs. 8 and 9 are similar results at a much higher frequency (i.e. Γ= 10). No phenomelogical differences exist between these two cases; only the detailed structure of the individual distribution differ.

The effort of this report has been toward trying to understand the effect of the non-homogeneous transition upon the energy exchange between the solid and the fluid. In order to simplify the analysis, it has been assumed that no longitudinal damping is present in either the elastic layer or the transition layer; since this analysis deals only with longitudinal displacements and stresses, any damping in the shearing modes will not effect these results. In addition, the density of the solid and of the transition layer has been assumed to equal the density of water; this is a very reasonable assumption for the coating materials of interest.

IV- CONCLUSIONS

The effect of a small transition layer, interposed between a compliant surface and the fluid, on the propagation of the longitudinal waves generated at the lower boundary of the coating has been studied. The transition layer has been assumed to be a non-homogeneous layer with properties ranging from that of the solid at the lower end to that of the fluid at the upper end. At the lower frequencies the coating disturbances have very long wavelengths such that not only is the transition layer transparent to these disturbances, but the coating itself is also transparent. The presence of the solid-fluid interface becomes noticeable at the higher frequencies where the disturbance wavelength becomes a noticeable fraction of the coating thickness. At the higher frequencies, the coating can exhibit resonance conditions similar to a closed-closed or a closed-open pipe. For fluid wave speeds greater than the solid wave speed, a closed-closed condition can be obtained while for a fluid wave speed less than the solid wave speed, a closed-open pipe resonance is obtained.

The particle displacement overshoot profile depends not only on the frequency of excitation, but also on the ratio of the coating to fluid properties. The magnitude of the overshoot due to the presence of the transition layer, for the conditions considered in this report, is not as predominant as in the case of the coating shear wave study. The stress distribution within the coating and the transition layer is monotonic and its general characteristics are not very sensitive to the conditions considered.

V - REFERENCES

1 - M. Pierucci, P. A. Baxley, "Compliant-Coating-Fluid Interaction: Coating Shear Waves in Stationary Fluid," AE&EM TR-82-03, S.D.S.U., 1982.

2 - Foundations of Solid Mechanics, Y. C. Fung, Prentice-Hall Inc., 1965.

3 - Fundamentals of Acoustics, L. E. Kinsler & A. R. Frey, Wiley & Sons, 1962.

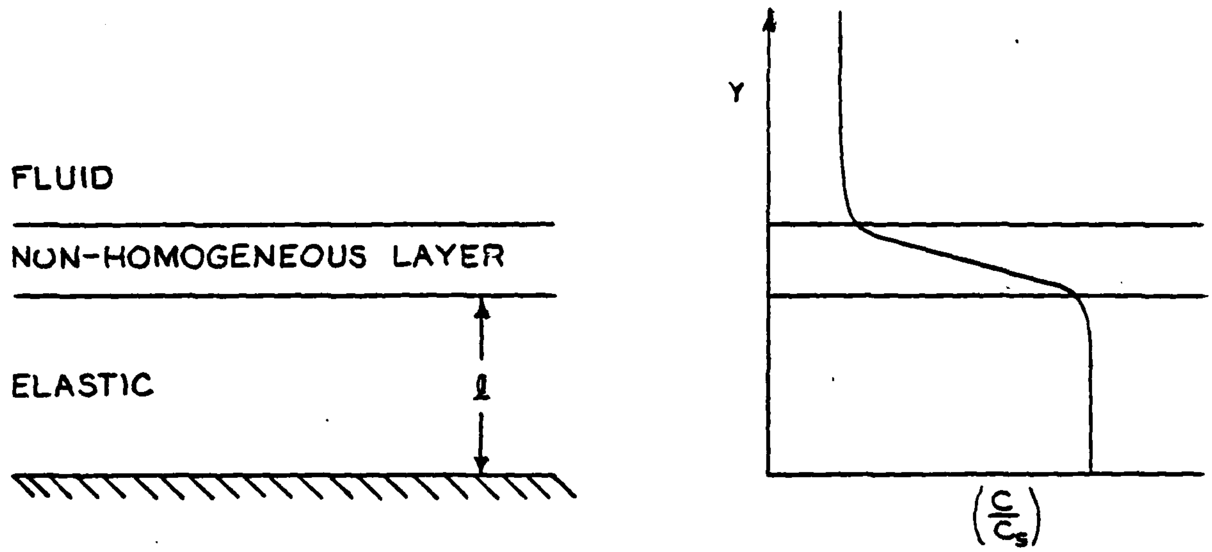

FIG.1- SOLID — TRANSITION LAYER — FLUID MODEL.

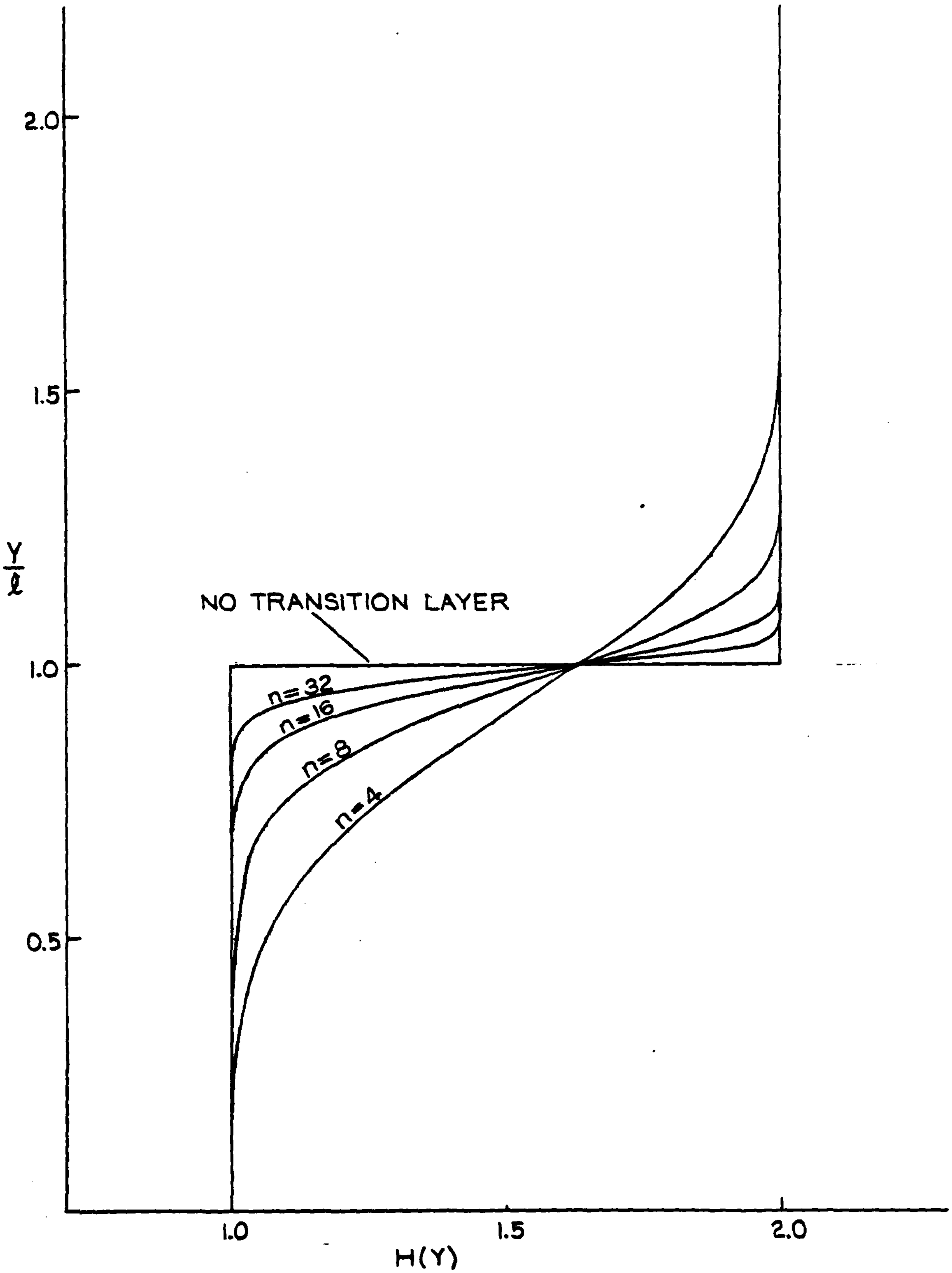

FIG. 2 - EFFECT OF PARAMETER n UPON THICKNESS OF TRANSITION LAYER. R=2.

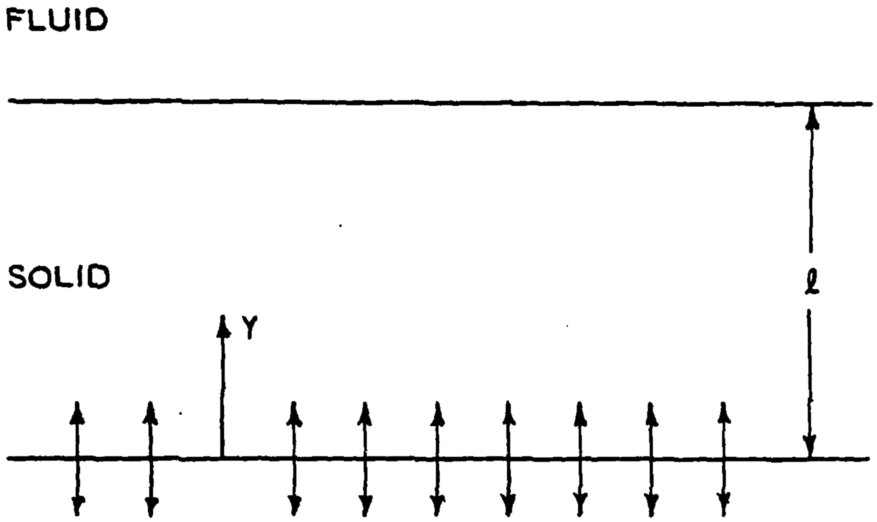

FIG. 3 – LONGITUDINAL WAVE PROPAGATION FROM SOLID TO FLUID. NO TRANSITION LAYER.

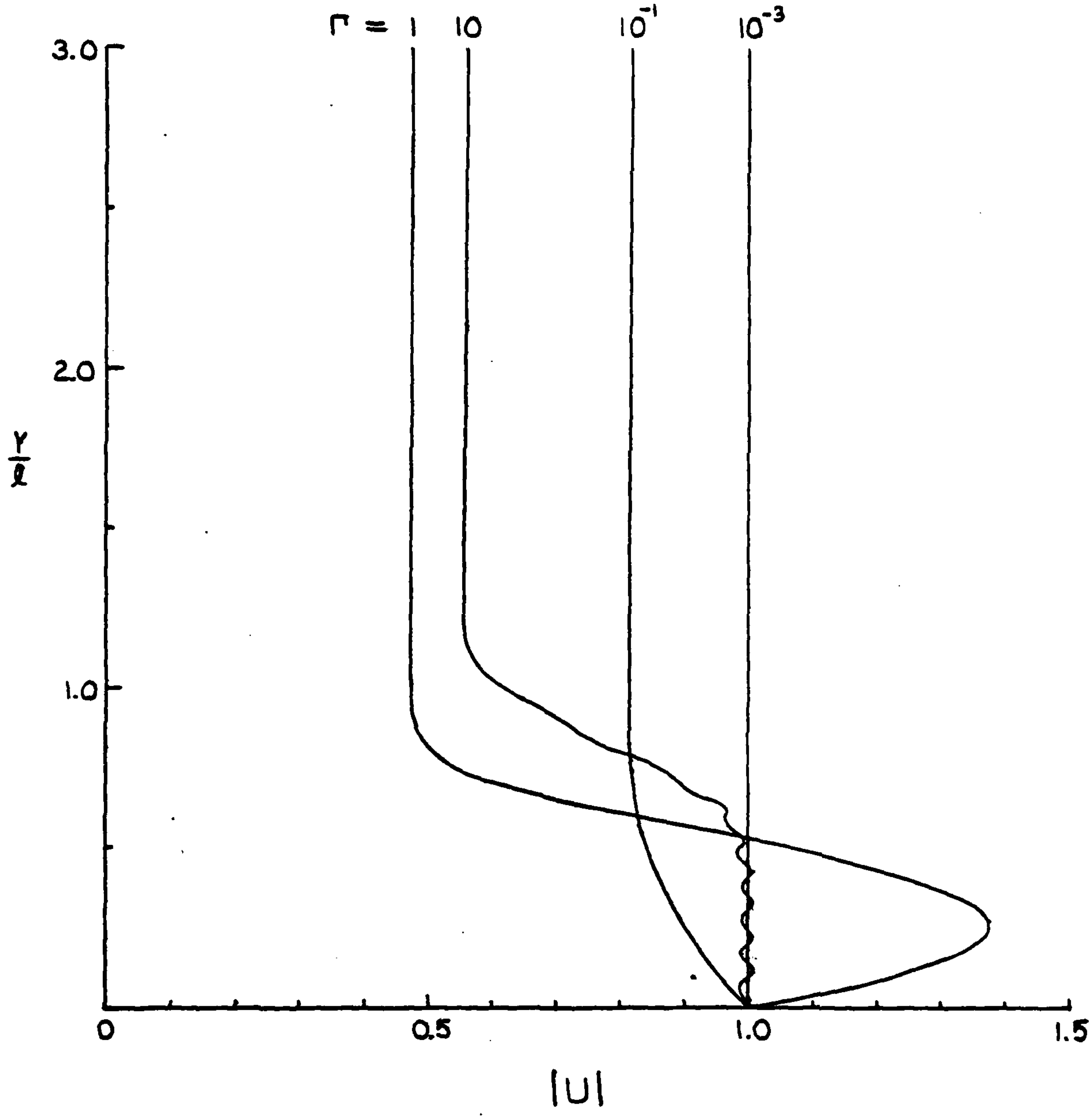

FIG. 4 - PARTICLE DISPLACEMENT DISTRIBUTION FOR DIFFERENT FREQUENCIES. n=8, R=10.

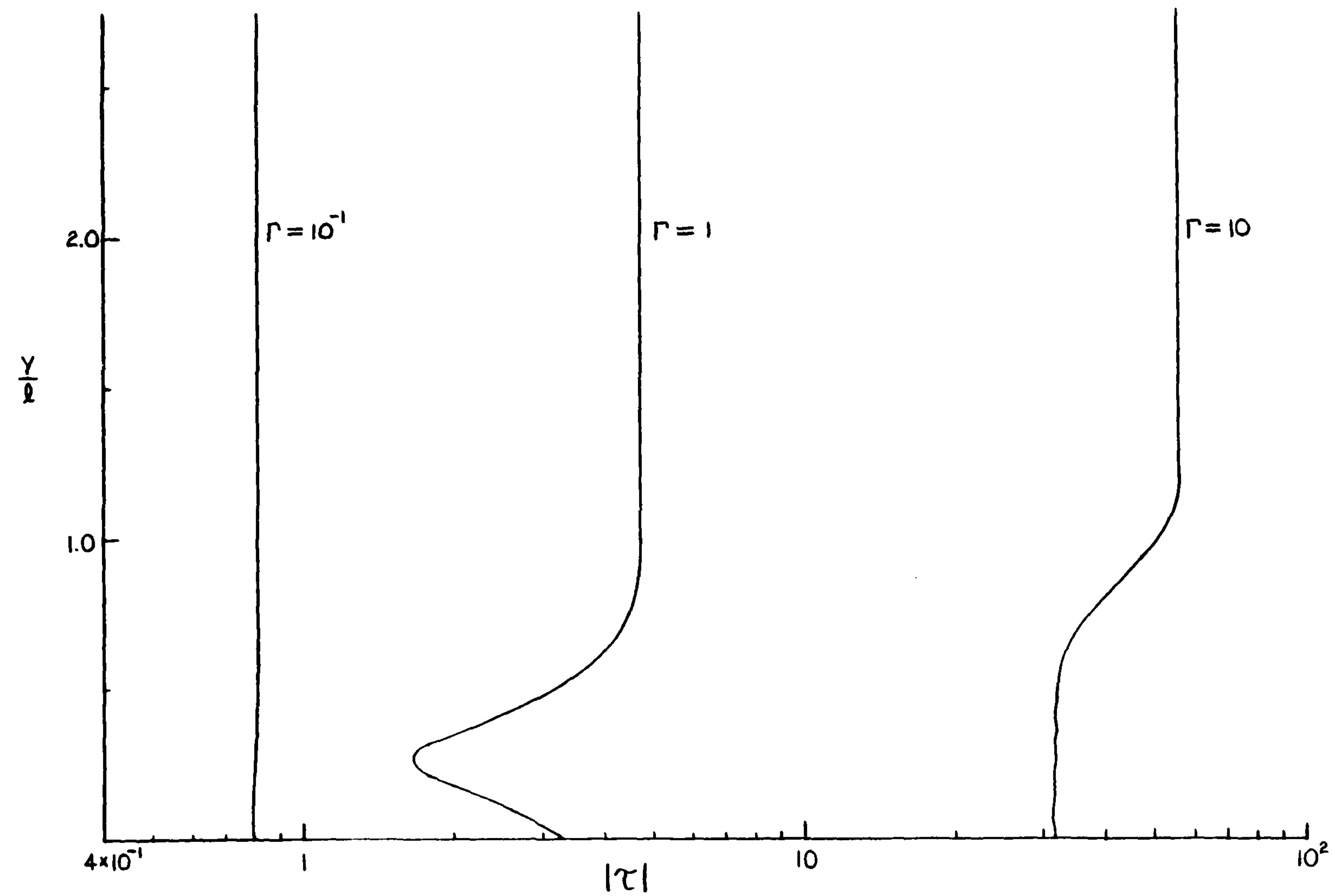

FIG. 5 – STRESS DISTRIBUTION FOR DIFFERENT FREQUENCIES. n=8, R=10.

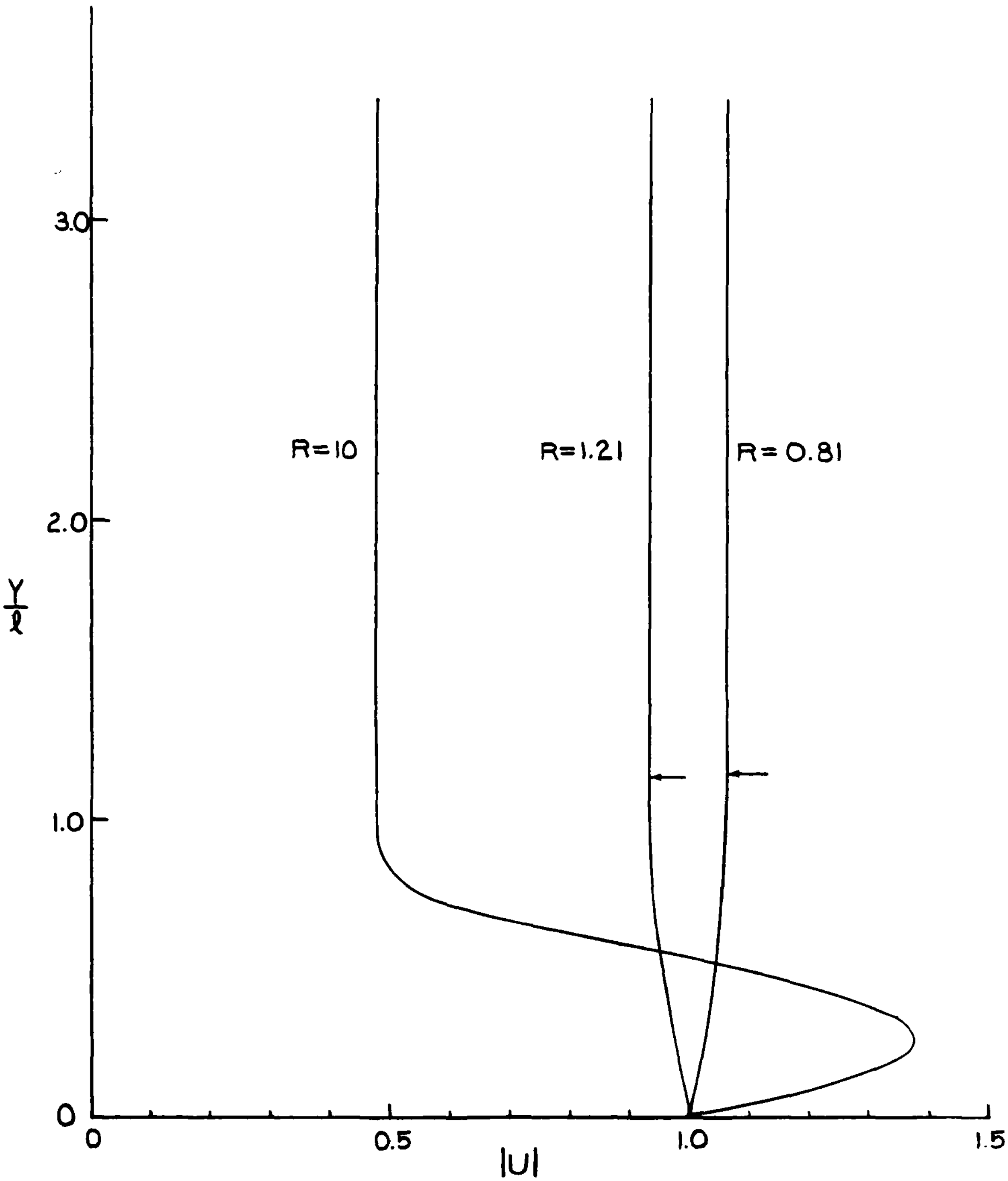

FIG.6 - VARIATION OF LONGITUDINAL PARTICLE DISPLACEMENT FOR DIFFERENT RATIOS OF PROPAGATIONAL VELOCITIES. $n=8, \Gamma=1$.
⟵ OUTER EDGE OF TRANSITION LAYER.

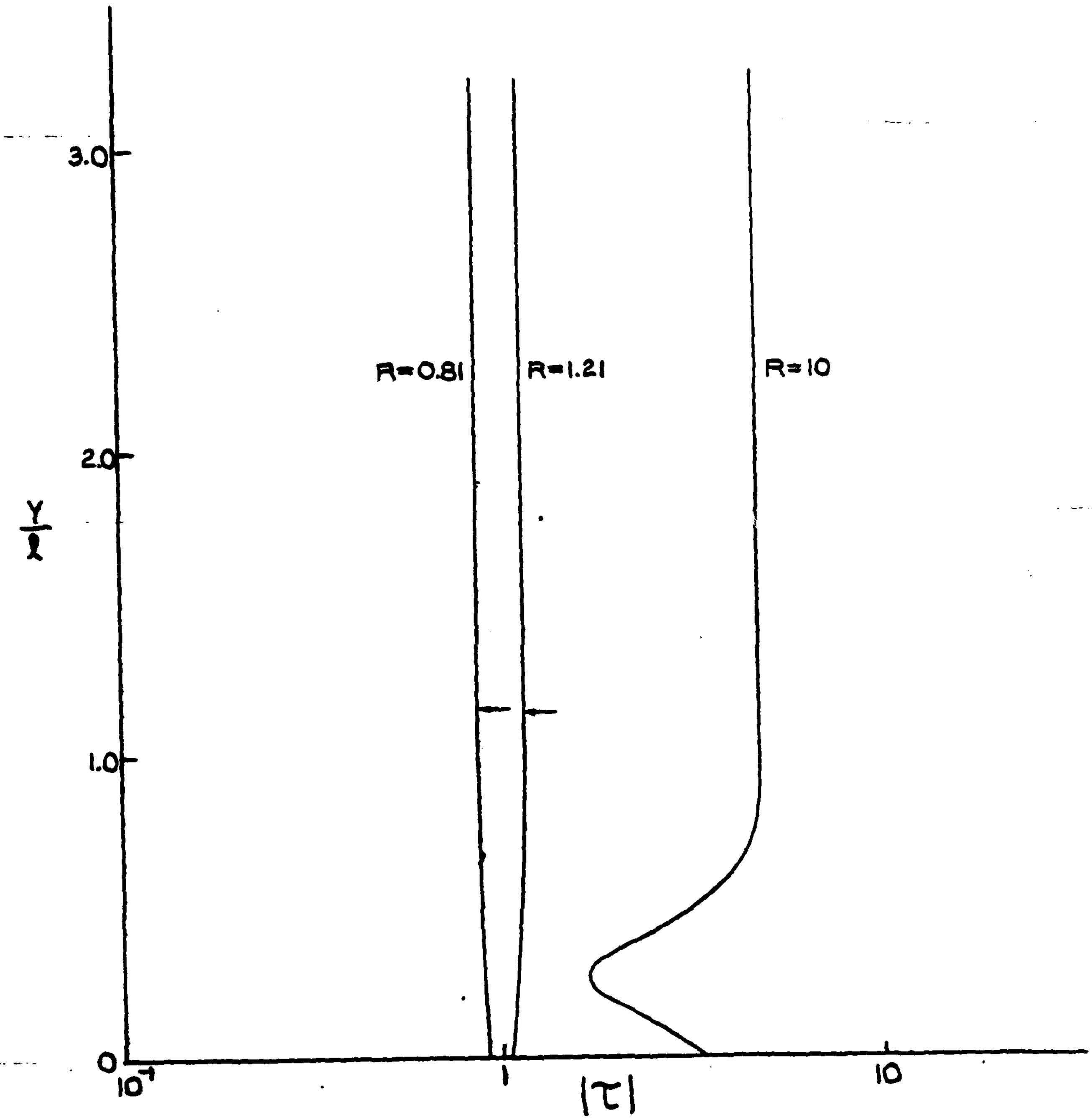

FIG.7 – VARIATION OF LONGITUDINAL STRESS DISTRIBUTION FOR DIFFERENT RATIOS OF PROPAGATIONAL VELOCITIES. $n=8, \Gamma=1$.

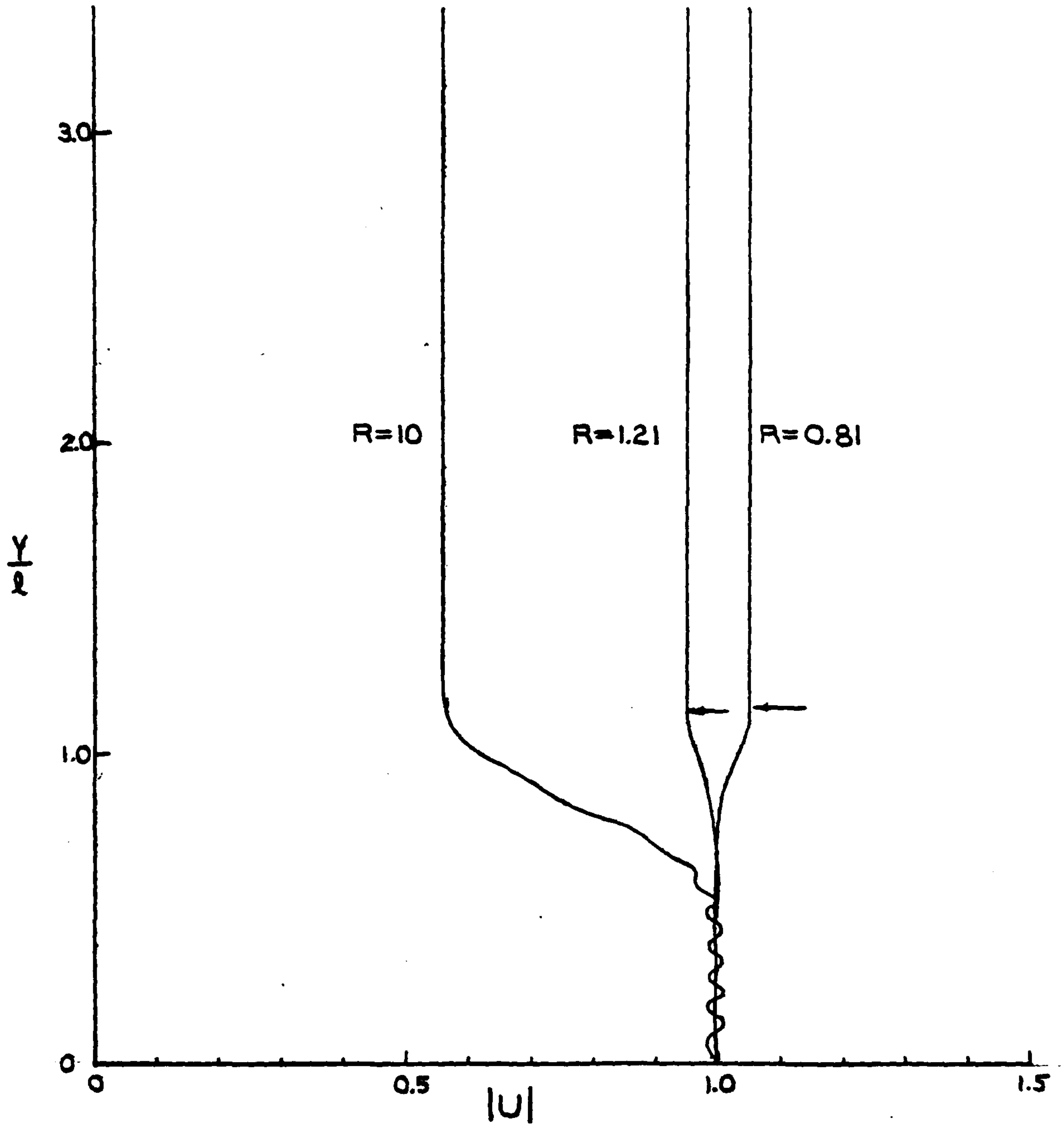

FIG.8 – VARIATION OF LONGITUDINAL PARTICLE DISPLACEMENT FOR DIFFERENT RATIOS OF PROPAGATIONAL VELOCITIES. $n=8, \Gamma=10$.

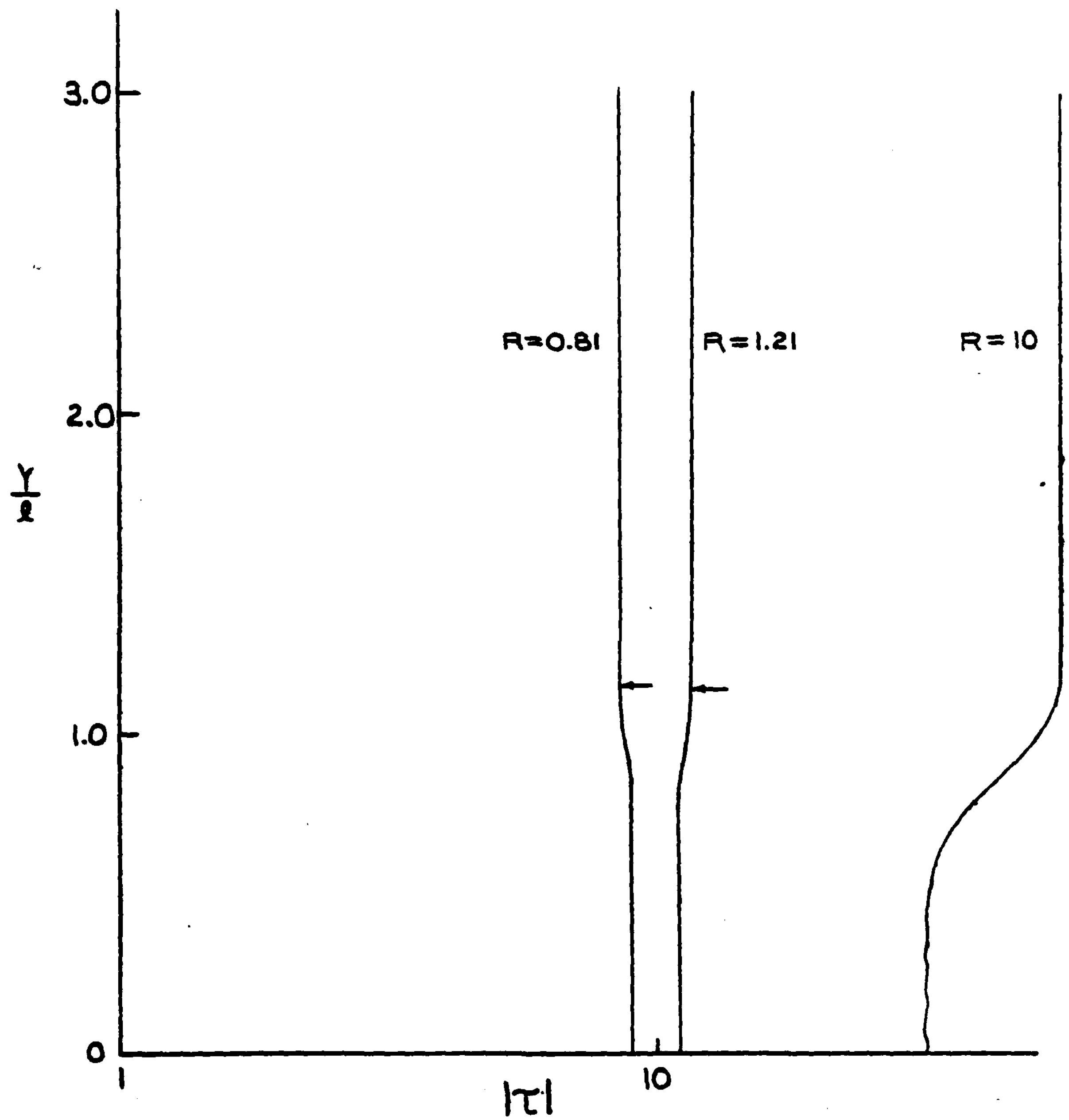

FIG. 9 - VARIATION OF LONGITUDINAL STRESS DISTRIBUTION FOR DIFFERENT RATIOS OF PROPAGATIONAL VELOCITIES. $n=8, \Gamma=10$.

APPENDIX

Enclosed are additional figures of particle displacement and shear stress distribution.

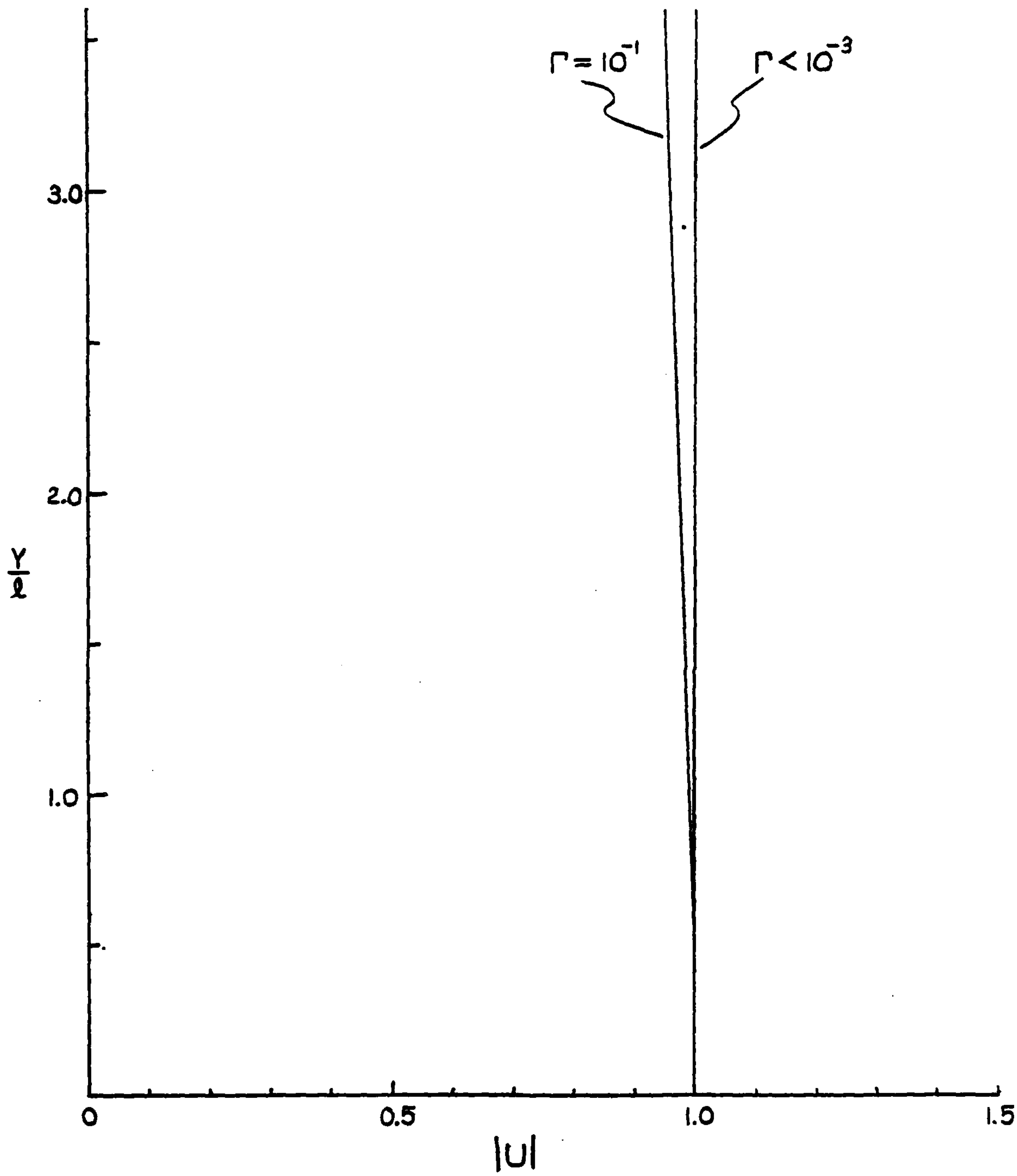

FIG. A-1 – PARTICLE DISPLACEMENT DISTRIBUTION FOR DIFFERENT FREQUENCIES. $n=8$, $R=0.25$.

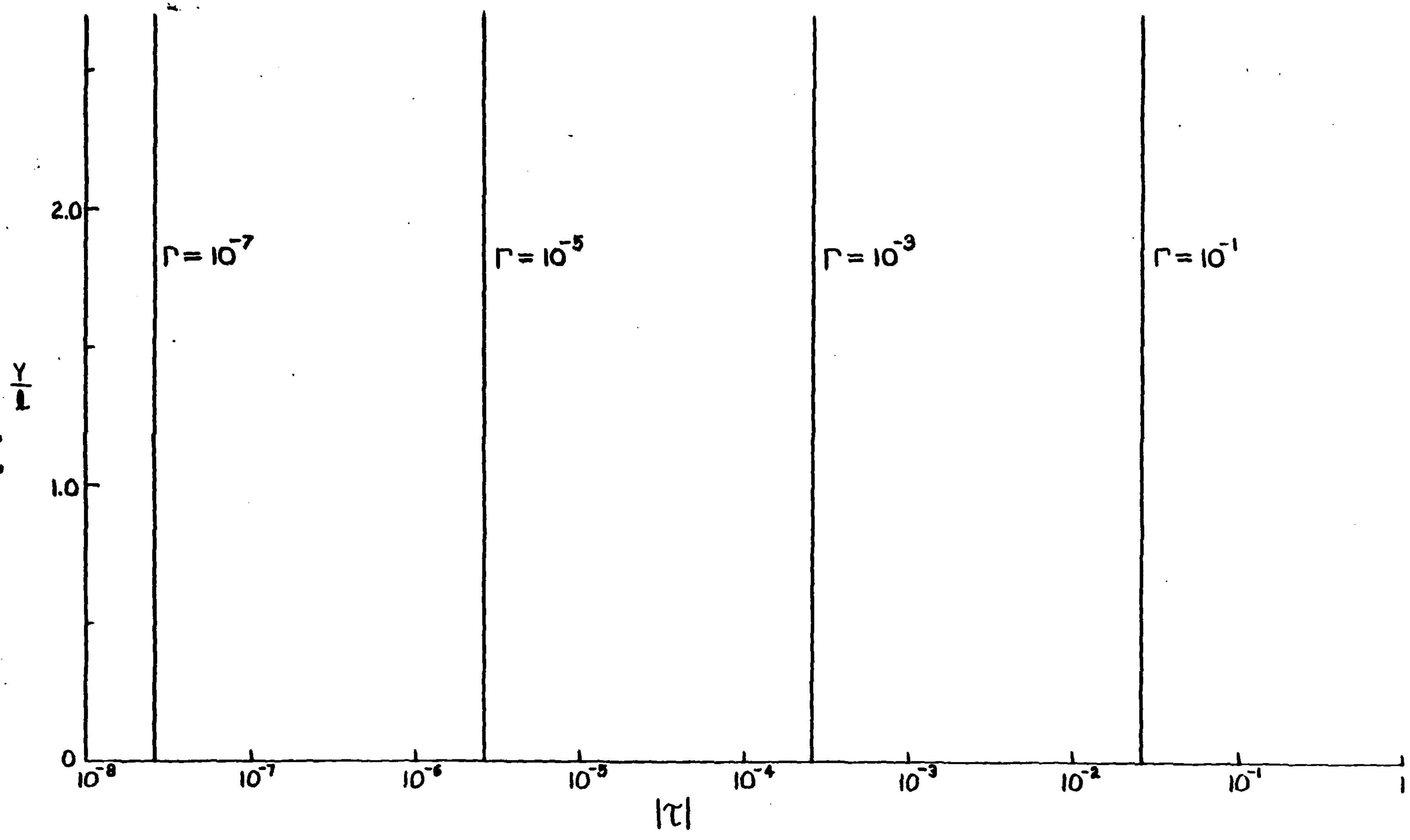

FIG. A-2 - STRESS DISTRIBUTION FOR DIFFERENT FREQUENCIES. $n=8$, $R=0.25$

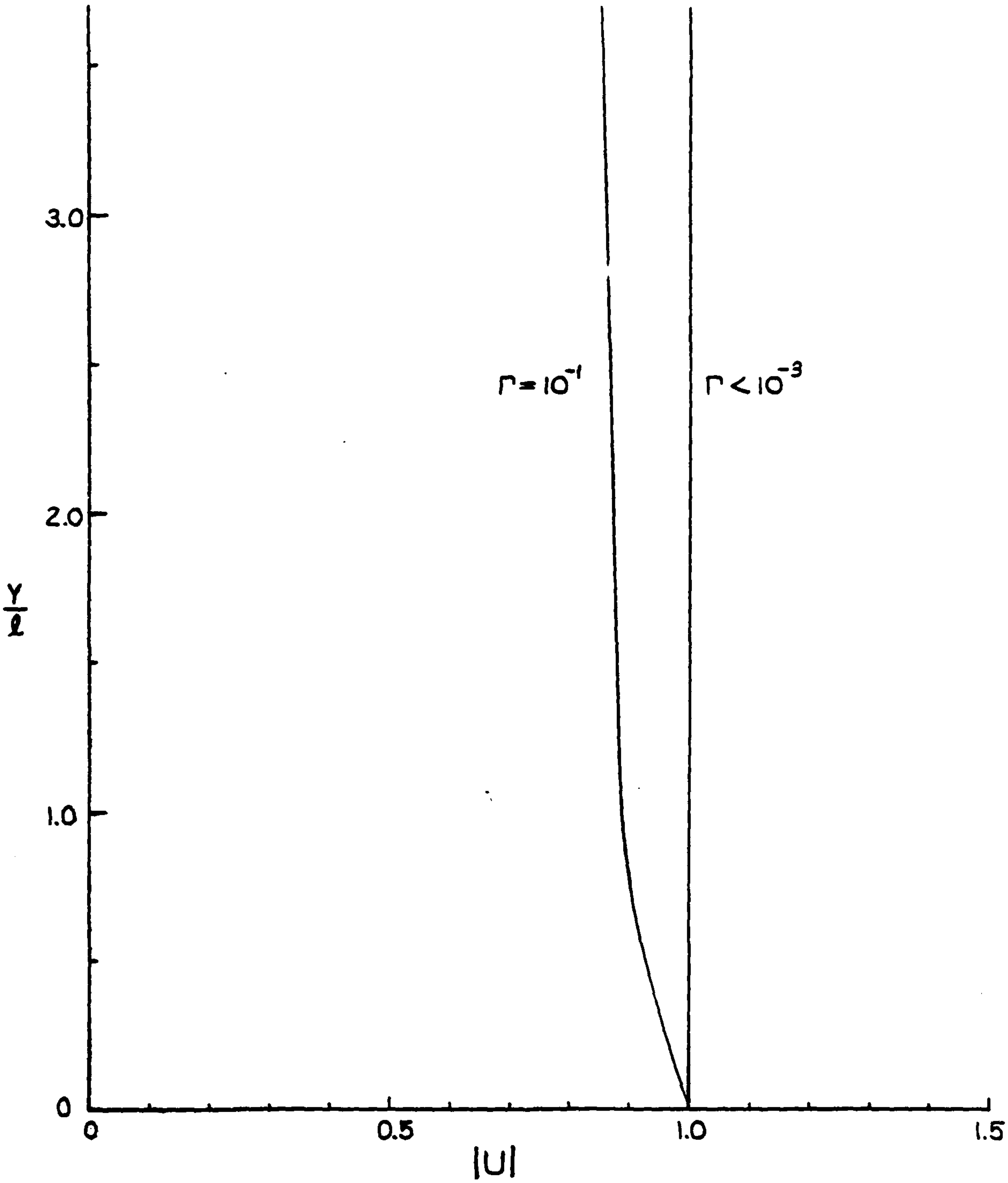

FIG. A-3 – PARTICLE DISPLACEMENT DISTRIBUTION FOR DIFFERENT FREQUENCIES. n=8, R=4.

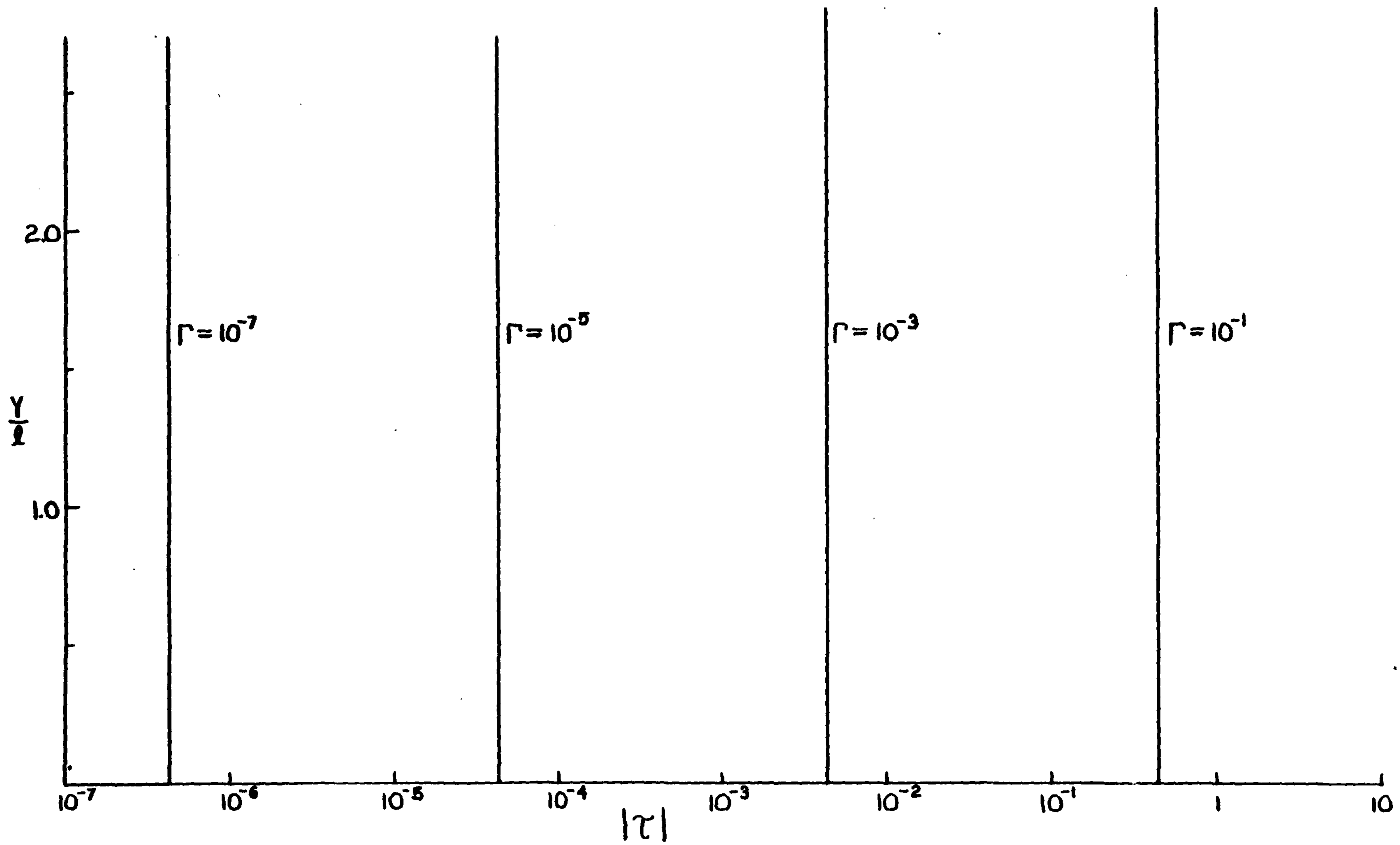

FIG. A-4 – STRESS DISTRIBUTION FOR DIFFERENT FREQUENCIES. $n=8$, $R=4$.

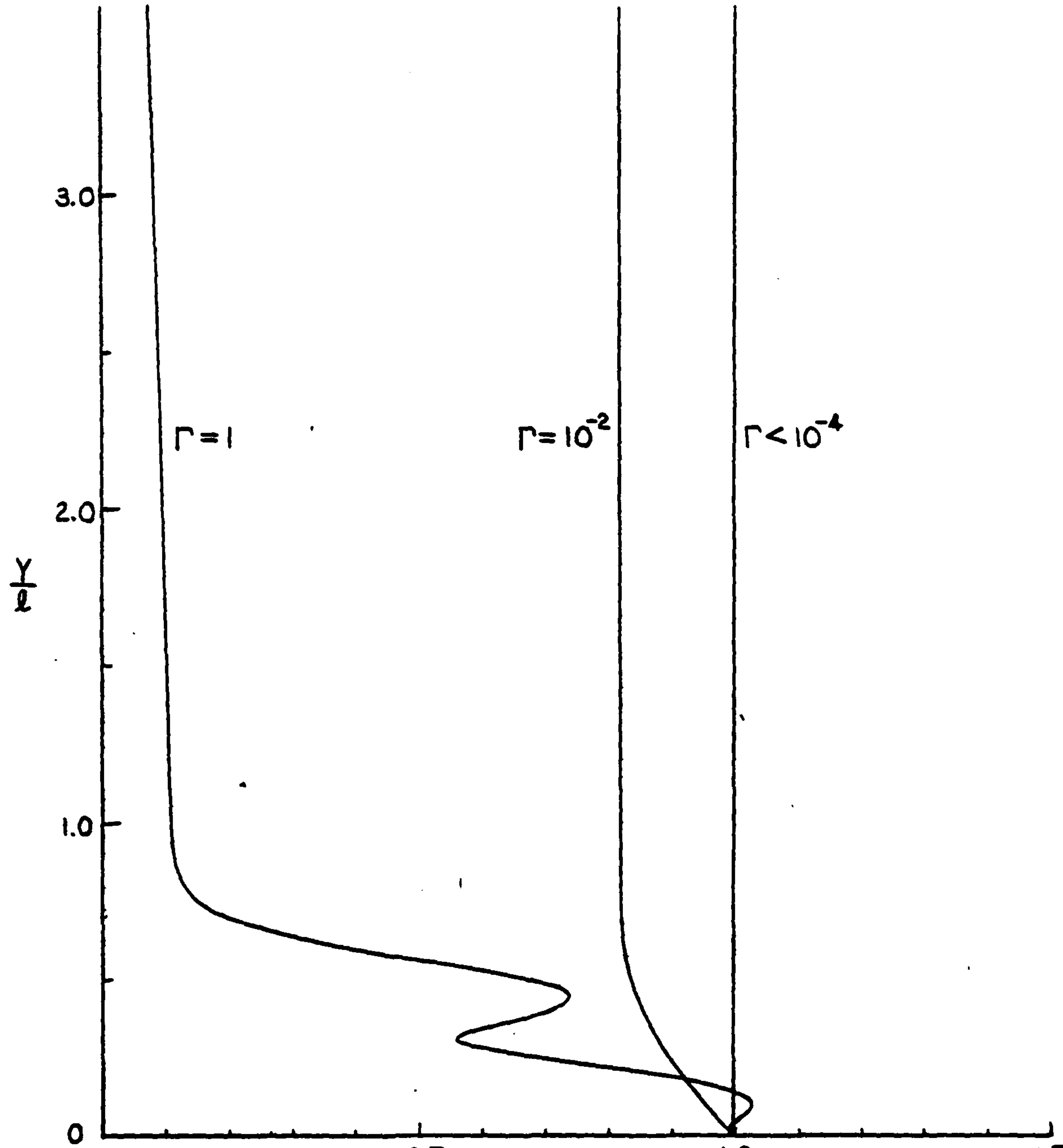

FIG. A-5 - PARTICLE DISPLACEMENT DISTRIBUTION FOR DIFFERENT FREQUENCIES. n=8, R=100.

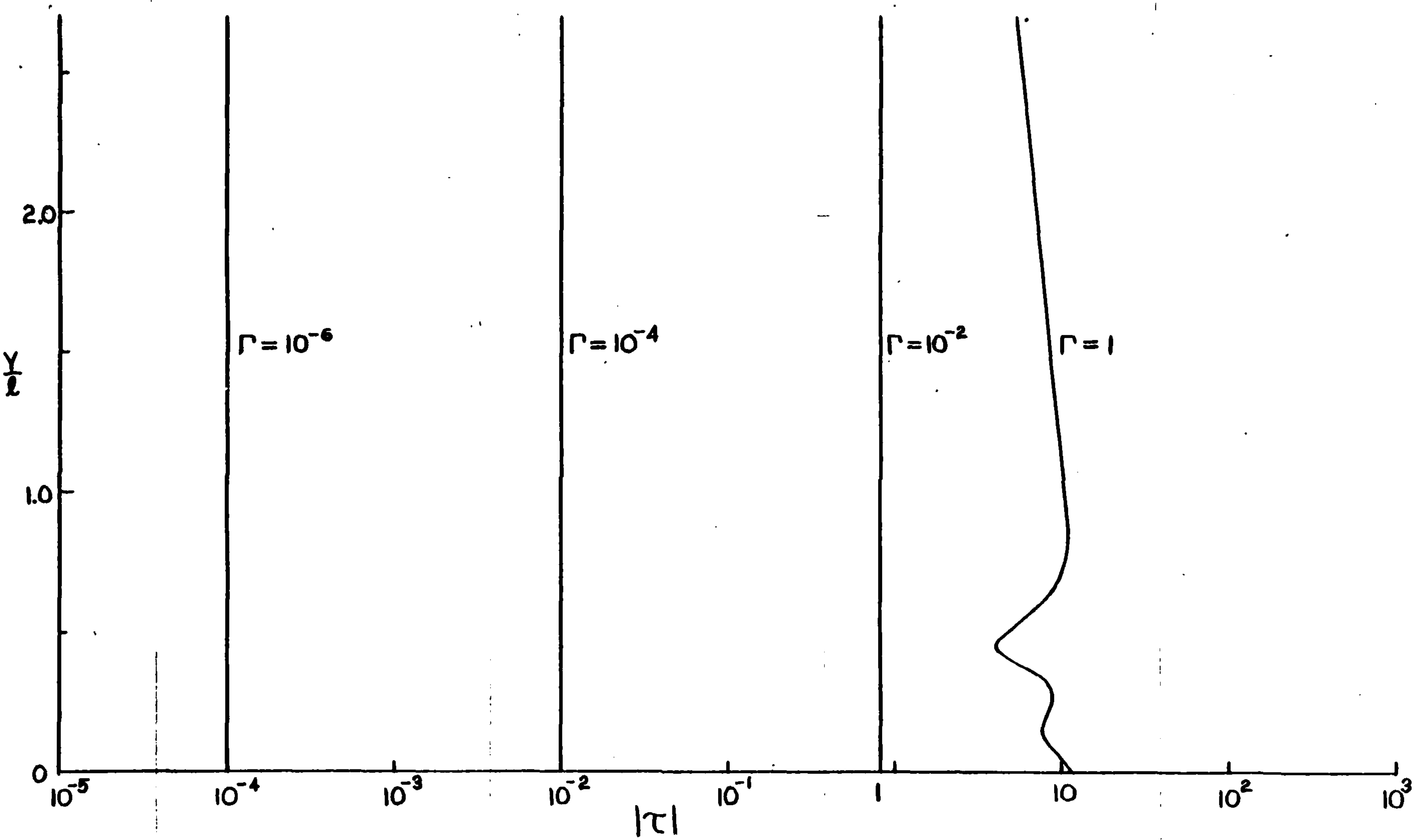

FIG. A-6 – STRESS DISTRIBUTION FOR DIFFERENT FREQUENCIES. $n=8, R=100$.

Unclassified
SECURITY CLASSIFICATION OF THIS PAGE (When Data Entered)

REPORT DOCUMENTATION PAGE		READ INSTRUCTIONS BEFORE COMPLETING FORM
1. REPORT NUMBER AE&EM TR-82-04	2. GOVT ACCESSION NO. AD-A111 274	3. RECIPIENT'S CATALOG NUMBER
4. TITLE (and Subtitle) Compliant-Coating-Fluid Interaction: Coating Longitudinal Waves in Stationary Fluid		5. TYPE OF REPORT & PERIOD COVERED Final Report March 1981-February 1982
		6. PERFORMING ORG. REPORT NUMBER AE&EM TR 82-04
7. AUTHOR(s) Mauro Pierucci Paul A. Baxley		8. CONTRACT OR GRANT NUMBER(s) N00014-81-K-0424
9. PERFORMING ORGANIZATION NAME AND ADDRESS Aerospace Engineering & Engineering Mechanics San Diego State University San Diego, CA 92182		10. PROGRAM ELEMENT, PROJECT, TASK AREA & WORK UNIT NUMBERS ONR 062-693
11. CONTROLLING OFFICE NAME AND ADDRESS Department of the Navy Office of Naval Research, Fluid Dynamics Div. Arlington, Virginia 22217		12. REPORT DATE February 1982
		13. NUMBER OF PAGES 21 + 7 Appendix Pages
14. MONITORING AGENCY NAME & ADDRESS(if different from Controlling Office)		15. SECURITY CLASS. (of this report) unclassified
		15a. DECLASSIFICATION/DOWNGRADING SCHEDULE

16. DISTRIBUTION STATEMENT (of this Report)

Approved for public release - distribution unlimited.

17. DISTRIBUTION STATEMENT (of the abstract entered in Block 20, if different from Report)

18. SUPPLEMENTARY NOTES

19. KEY WORDS (Continue on reverse side if necessary and identify by block number)

Longitudinal waves; fluid-structure interactions; compliant coating; transition layer; non-homogeneous layer.

20. ABSTRACT (Continue on reverse side if necessary and identify by block number)

The presence of a thin non-homogeneous layer at the interface of an elastic and a fluid medium can alter the energy exchange between the two media. In this report the effect of the transition layer upon the propagation of one-dimensional longitudinal waves is analyzed. The motion of the lower boundary of the elastic layer is assumed known and the energy radiation into the fluid is obtained.

DD FORM 1473, 1 JAN 73 EDITION OF 1 NOV 65 IS OBSOLETE
S/N 0102-LF-014-6601

Unclassified
SECURITY CLASSIFICATION OF THIS PAGE (When Data Entered)

END

DATE

FILMED

03-82

DTIC